

1  
2  
3  
4  
5  
6  
7  
8  
9  
10  
11  
12  
13  
14  
15  
16  
17  
18  
19  
20  
21

**The formation of chromatin domains:  
a new model**

Giorgio Bernardi  
[gbernardi@uniroma3.it](mailto:gbernardi@uniroma3.it)

Science Department, Roma Tre University, Viale Marconi 446, 00146 Rome, Italy, and  
Stazione Zoologica Anton Dohrn, Villa Comunale, 80121 Naples, Italy.

## 22 **Abstract**

23 The mechanisms of formation of LADs, the lamina associated domains, and TADs, the  
24 topologically associating domains of mammalian chromatin, were investigated here by using as  
25 a starting point the observation that chromatin architecture relies on an isochore framework and  
26 by doing a new analysis of both isochore structure and the isochore/chromatin domain  
27 connection. This approach showed that LADs correspond to isochores from the very GC-poor,  
28 compositionally very homogeneous L1 family and from the “low-heterogeneity” L2 (or L2<sup>-</sup>) sub-  
29 family; in fact, LADs are compositionally flat, flexible chromatin structures (because of the  
30 nucleosome depletion associated with the frequent oligo-A’s) that attach themselves to the  
31 nuclear lamina in self-interacting clusters. In contrast, TADs correspond to the increasingly GC-  
32 richer isochores from the “high-heterogeneity” L2 (or L2<sup>+</sup>) sub-family and from the H1, H2 and  
33 H3 families. These isochores, making the framework of the individual chromatin loops or of the  
34 chromatin loop ensembles of TADs, were found to consist of single or multiple GC peaks. The  
35 self-interacting single or multiple loops of TADs appear to be shaped by the property that  
36 accompany the increasing levels of GC and CpG islands in their isochore peak backbones,  
37 namely by an increasing bendability due to decreasing nucleosome density which is accompanied  
38 by decreasing supercoiling and increasing nuclease accessibility. In conclusion, chromatin  
39 architecture appears to be encoded and molded by isochores, the DNA units of genome  
40 organization. This “isochore encoding/molding model” of chromatin domains represents a  
41 paradigm shift compared to previously proposed models. Indeed, the latter only rely on the  
42 properties of architectural proteins, whereas the new model is essentially based on the physico-  
43 chemical properties of isochores and on their differential binding of nucleosomes.

44

## 45 **Introduction**

46 In interphase nuclei, chromatin comprises two sets of domains that are largely conserved  
47 in mammals: LADs, the lamina associated domains (~0.5Mb median size), that are scattered over  
48 all chromosomes and correspond to GC-poor sequences (1-3), and TADs, the topologically  
49 associating domains (0.2-2 Mb in size), a system of GC-rich loops (4-7); many TADs can be  
50 resolved into contact domains (0.185 Mb median size (6)).

51 In spite of the recent, impressive advances in our understanding of chromatin domains  
52 (see refs. 8-14, for reviews), the problem of their formation mechanism(s) is still unsolved.  
53 Interesting models have been proposed (15-24), but no satisfactory solution has been reached so  
54 far. The currently predominant model for TAD formation is the “chromatin extrusion model”  
55 (18,19), which proposes that TADs emerge as a consequence of loop extrusion by loop extruding  
56 factors (including cohesin), which is limited by boundary elements (including CTCF).

57 Here, the problem of chromatin domain formation was approached by taking into account  
58 the observation that isochores (see ref. 25 for a review) make up the framework of chromatin  
59 domains (26) and by having a new look at isochore structure and at the isochore/chromatin  
60 domain connection. This approach was applied to human chromosome 21 which was chosen  
61 because 1) this chromosome is a good representative of human chromosomes, allowing an  
62 extension of the results to all other chromosomes (as investigated in ref. 26); and 2) is the  
63 smallest human chromosome, allowing a more expanded graphical presentation of data.

64 As far as nomenclature is concerned, although TADs comprise, by definition, all the  
65 topologically associating domains, in the context of this article TADs will indicate the chromatin  
66 domains other than LADs. The main reason for this choice is that the mechanisms of formation  
67 of the two sets of domains are different, even if based on the same fundamental DNA property.

68  
69

70 **Results**

71 *Isochore structure: a new analysis*

72 Figure 1A shows the compositional profile of the DNA sequence from human  
73 chromosome 21 as seen through non-overlapping 100Kb windows. This window size was used  
74 because 100KB is a plateau value under which the composition of DNA segments show an  
75 increasing variance with decreasing size (27) due to several factors (for instance, the distribution  
76 of interspersed repeated sequences).

77 Figures 1B and 1C display the isochore profile as obtained from the chromosome 21  
78 sequence using either a sliding window approach (28,29; Fig. 1B) or a fixed window approach  
79 (27, 30; Fig. 1C). Both approaches flatten the compositional profiles by averaging, in two  
80 different ways, the fluctuating values of the large regions characterized by “fairly homogeneous”  
81 composition, the isochores. In the case of the sliding window approach, remnants of the  
82 fluctuations can still be seen as small spikes in GC-rich regions, whereas in the case of the fixed  
83 window approach the fluctuations disappear because of the strict averaging procedure applied.

84 A new, simpler, in fact elementary, approach was used here, namely plotting the  
85 individual GC values of 100Kb DNA blocks as points. This approach was suggested by two  
86 recent results: 1) correlations hold between isochore properties and the properties of chromatin  
87 domains (31); and, more precisely, 2) the framework of TADs and LADs is made up by GC-rich  
88 and GC-poor isochores, respectively (26). One may therefore imagine a possible topological  
89 similarity between the flat structure of LADs and the loops of TADs on the one hand, and the  
90 compositionally flat GC-poor and the compositionally heterogeneous GC-rich isochores,  
91 respectively, on the other. If such is the case, clearly a simple 100Kb point-by-point profile of  
92 GC levels is preferable not only to both sliding and fixed window approaches, that flatten the  
93 compositional profile, but also to the color bar plot of 100Kb DNA segments (Fig. 1A) for  
94 graphical clarity reasons.

95           The point-by-point profile (see Fig. 1D) expectedly showed the compositionally flat  
96 region 2 and the H1 and L2 peaks (**a** to **f**) of regions 1 and 3, that were already evident in Figs.  
97 1A, 1B and 1C. It also led, however, to the discovery that the sequences of isochores from H1  
98 (region 4), H2 (region 5) and H3 (region 6) isochores were not simply fluctuating within the  
99 compositional borders of the corresponding families (see Supplementary Table S1), but  
100 consisted, in fact, of sets of GC peaks. Upon close inspection, these very evident peaks may be  
101 seen to correspond to the minute peaks of Fig. 1B, that were flattened by the sliding window  
102 approach. Expectedly, the peaks of the point-by-point plots covered a broader GC range  
103 compared with the flattened peaks of the sliding window approach, as shown by comparing Fig.  
104 1D with Fig. 1B, and Fig. 1F with Fig. 1E (the high resolution compositional profiles of a multi-  
105 peak H2 isochore from chromosome 20).

106           In purely compositional terms (see Fig. 2 for a larger-scale presentation of the data of Fig.  
107 1D), three different situations were found: 1a) a series of single peaks (regions 1 and 3)  
108 corresponding to an H1 isochore (**a**), and to several L2 isochores (**b** to **f**), in which latter case  
109 very few points were slightly beyond the “fixed” isochore family borders, but still within the  
110 “extended” borders of Supplementary Table S1; 1b) several very sharp H3 single peaks (region  
111 6) that included sequences belonging to the H2 and even to the H1 family, in which case an  
112 overall GC range of 18% was reached; 2) a very homogeneous L1 isochore (region 2), in which  
113 the overall GC range barely reached 4% and all points were within the “fixed” GC borders of  
114 isochore family L1; and 3) two series of GC-rich multi-peak isochores that belonged to H1  
115 (region 4) and H2 (region 5) families in which, again, very few points were slightly beyond the  
116 “fixed” isochore family borders. The striking difference between the compositional profile of L1  
117 and H3 isochores is shown in Fig. 2A. Expectedly, when using a higher resolution windows  
118 (50Kb; see Supplementary Figure S1) the compositional profiles of isochore peaks became

119 broader in the GC level gradients and more complex, because of the presence of interspersed  
120 repeated sequences and CpG islands (see ref. 27).

121

### 122 *Isochores and LADs*

123 It is well established (see refs. 1-3) that LADs 1) may cover ~35% of the human genome;  
124 2) comprise 1,100-1,400 discrete domains demarcated by CTCF sites and CpG islands; 3) have a  
125 median size of ~0.5Mb; 4) are scattered over all chromosomes; 5) can be subdivided into cLADs,  
126 *i.e.*, “constitutive” LADs present in the four cell types originally tested and fLADs “facultative”  
127 LADs, only present in some cell types (in fact, only ~15% of the genome is involved in “stable  
128 contacts” present in most cells); 6) are characterized, in the case of cLADs, by conserved  
129 positions in syntenic regions of human and mouse chromosomes; 7) show a correspondence of  
130 cLADs and ciLADs (the “constitutive inter-LADs”) with GC-poor and GC-rich isochores,  
131 respectively.

132 As shown in Figs. 3A (and 4A,4B), the major LAD of chromosome 21 corresponds to a  
133 large L1 isochore (which, incidentally, includes an exceptional GC-poor interLAD; see also the  
134 interval in the self-interacting domains corresponding to the L1 isochore in Fig. 4C). The other  
135 LADs correspond to the L1 isochores that separate the L2 peaks (to be described below and in  
136 the following section), and to a “valley” L2 isochore comprised between two H1 isochores (on  
137 the right side of Fig. 3A). Moreover, two LADs flank the centromere; in fact, this appears to be  
138 the rule for all human chromosomes, as judged by looking at the results of ref. 26.

139 In chromosome 20 (Fig. 3B), the largest LAD corresponds to an L2 isochore (interrupted  
140 by an interLAD) while several other LADs correspond to L2 valley isochores flanked by H1  
141 isochores; among faint LADs, one (extreme right) corresponds to an H1 isochore comprised  
142 between two H2 isochores and two other ones flank the centromere. In the very GC-rich

143 chromosome 19 (Fig. 3C), two LADs correspond to two H1 isochores flanking an H2 isochore  
144 and two other LADs correspond to L2 isochores flanking an H1 isochore; finally, two faint LADs  
145 flank the centromere.

146 These results show that LADs correspond not only to L1 isochores that represent ~19% of  
147 the genome (incidentally, not too far from the ~15% involved in “stable contacts”; see ref. 3), but  
148 also to L2 isochores and even to H1 isochores in the rare case of very GC-rich chromosomes.

149 As far as L2 isochores are concerned, it appears (see Supplementary Table 1 and Fig. 1)  
150 that 1) some isochores belong to a “low-heterogeneity” L2 sub-family that may be called  $L2^-$ ,  
151 show a flat profile (see, for example, the largest LAD of chromosome 20); and 2) some other  
152 isochores belong to a “high-heterogeneity” L2, or  $L2^+$ , sub-family that are higher in average GC  
153 and are in the shape of single peaks (see Figs. 1 A-D and 3A). Now, as shown in Fig. 3,  $L2^-$   
154 isochores correspond to LADs, whereas  $L2^+$  isochores correspond to interLADs and TADs (see  
155 the following section). The remaining L2 isochores are generally present as valleys flanked by  
156 GC-richer isochores (see Fig. 3A,3B,3C; the relative amounts of L2 sub-families are presented in  
157 Supplementary Table S1).

158

### 159 *Isochores and TADs*

160 It should be recalled, as a preliminary remark, that the isochores from the five families  
161 (L1, L2, H1, H2 and H3) of the human genome (and other mammalian genomes; 32) are  
162 characterized not only by increasing GC levels and different short-sequence frequencies, but also  
163 by increasing compositional heterogeneities, increasing levels of CpG, CpG islands and Alu  
164 sequences and by decreasing levels of LINE sequences and of 5mC/CpG ratios (27,33-37).  
165 Moreover, at the chromatin level, GC increases are correlated with higher bendability (38),

166 higher nuclease accessibility (39,40), lower nucleosome density (41) and lower supercoiling  
167 (42,43), all properties linked to DNA sequences.

168 The connection of the isochores of chromosome 21, as seen in Figs. 1D and 2, with  
169 chromatin loops can be described as follows (see Fig. 4A,4B,4C): 1) regions 1 and 3 show a  
170 series of H1 (a) and L2 (b to f) isochores in which latter case at least some of their single peaks  
171 appear to correspond to individual self-interactions; 2) region 2 is the GC-poorest L1 isochore  
172 which corresponds to two self-interactions (separated by an exceptional interLAD); 3) the multi-  
173 peak H1 isochores of region 4 correspond to a large interLAD region and to several self-  
174 interactions; the two short sequences X and Y, corresponding to LADs, separate region 4 from  
175 regions 3 and 5; 4) the small multi-peak H2 isochore (region 5) seems to correspond to a single  
176 self-interaction; this may be due to the dense packing of the peaks and/or to a lack of resolution;  
177 5) a series of H3 isochores (red points comprised between two red arrows) correspond to a series  
178 of self-interactions comprised between the two red lines on the heat map; in this case, the six H3  
179 isochore peaks correspond to at least three chromatin loops. In conclusion, the two classes of  
180 isochores, single-peak and multi-peak, essentially correspond to two classes, single-loop and  
181 multi-loop, respectively, of TADs (both of which also show inter-chromosomal interactions; 26).

182 The correspondence between isochores peaks and self-interactions is improved at a higher  
183 resolution of the heat map (compare the high-resolution Fig. S2A with the low resolution Fig.  
184 S2B). Likewise, a very good match of isochore peaks with chromatin loops can be seen in the  
185 high resolution heatmap of the multipeak H2 isochore of chromosome 20 (see Supplementary  
186 Fig. S3).

187 A very interesting correlation is shown in Fig. 4D, in that regions 1 and 3 to 6 correspond  
188 to A compartments (open chromatin) whereas region 2 and the short X and Y sequences  
189 correspond to B compartments (closed chromatin; see ref. 15). More precisely, the A



190 compartment corresponds to multi-peak isochore TADs (regions 1,3,4,5,6), the B compartment to  
191 individual LADs (region 2,X,Y), the former being more frequent in telomeric regions.

192

## 193 **Discussion and Conclusion**

### 194 *Encoding of chromatin domains by isochores*

195 Very recent investigations showed that GC-poor and GC-rich isochores should be  
196 visualized as the framework of chromatin architecture or, in other words, as the DNA units that  
197 underlie LADs and TADs, respectively (26). This was an important step towards the idea that  
198 isochores encode chromatin domains. The present results provide a conclusive evidence for this  
199 idea, by showing a precise match between the chromatin domains and the isochores of  
200 chromosome 21 and by generalizing these results to all human chromosomes.

201 Indeed, the compositional profiles, the heatmaps and the LAD maps (26) show that: 1) the  
202 isochores from the L1 family and the L2<sup>-</sup> sub-family correspond to LADs in all human  
203 chromosomes; 2) L2<sup>+</sup> peaks emerging from an L1 background and corresponding to interLADs  
204 and TADs are also found in other human chromosomes, although less frequently than in  
205 chromosome 21; likewise, H3 peaks also corresponding to interLADs and TADs are present in  
206 most human chromosomes; 3) the spikes of the compositional profiles of H1 and H2 isochores  
207 of Fig. 1B, that reflect the peaks of Fig. 1D, are regularly present in H1 and H2 isochores from all  
208 human chromosomes and correspond to the peaks of point-by-point profiles (Cozzi P. et al.,  
209 paper in preparation) and to heat map interactions. This general match is important in that the  
210 only alternative to the encoding proposed here is that the match of the thousands of LADs and  
211 TADs with the corresponding isochores is just a coincidence (and this cannot be *quia absurdum*).

212

### 213 *Molding of chromatin domains by isochores*

214           The present results also solve an important open problem, namely the mechanism of  
215           formation of chromatin domains. Indeed, LADs should be visualized as chromatin structures  
216           corresponding to GC-poor isochores that are flexible, because of the local nucleosome depletions  
217           linked to the richness of oligo-A sequences in the corresponding isochores (33,37,44,45; G.  
218           Lamolle, H. Musto, G. Bernardi; paper in preparation). LADs only twist and bend in order to  
219           adapt and attach themselves to (and even embed in) the lamina, which is reassembled after  
220           mitosis (3). Expectedly, this leads to self-interactions (see Fig. 4), as well as to interactions with  
221           other LADs from the same chromosomes (26; see, for example, the two LADs bracketed by  
222           black lines in Fig. 4). In the case of TADs, the GC gradient within each GC-rich isochore peak is  
223           accompanied by properties, increasing levels of CpG, CpG islands and Alu sequences, that lead  
224           to increasing nucleosome depletion and bendability and decreasing supercoiling (38-43). These  
225           factors constrain the corresponding chromatin to fold into loops.

226           The models for the formation of LADs and TADs developed in this investigation are  
227           presented in Fig. 5, which stresses a keypoint, namely the central role played by the  
228           compositional properties of isochores in the formation of chromatin domains. Indeed, the folding  
229           model presented here clearly relies on isochore sequences, their nucleosome depletion and the  
230           emerging local (in LADs) or extended (in TADs) flexibility of the chromatin fiber.

231           It should be stressed that this “isochore encoding/molding model” of chromatin domains  
232           represents a paradigm shift compared to previously proposed models. Indeed, the latter only rely  
233           on the properties of architectural proteins, whereas the new model is essentially based on the  
234           physico-chemical properties of isochores and on their differential binding of nucleosomes.

235           The “isochore encoding/molding model” of chromatin domains is, however, compatible 1)  
236           with both the requirements of CTCF binding to close chromatin loops into insulated TADs (46)  
237           and the lack of such requirements (47); 2) with the interaction of topoisomerase II beta with

238 cohesin and CTCF at topological domain borders (48); 3) with an “insulation-attraction model”  
239 of TAD formation (9) in which the insulation observed at TAD boundaries may result from  
240 stiffness of the chromatin fiber caused by functional elements (CTCF binding sites, highly active  
241 transcription starting sites etc) associated with increased nucleosome density and specific local  
242 chromatin interactions due to “attractive forces” (not better specified but possibly linked to  
243 supercoiling).

244

245 *The “isochore encoding/molding model” vs the “chromatin extrusion model”*

246 Although, “the extrusion model” could overlap with the “isochore encoding/molding  
247 model”, a question may be raised about which one of the two models is better supported by facts.  
248 An answer may come by considering what happens in the case of the “mitotic memory”, namely  
249 the rapid and precise re-establishment of the original interphase chromatin domains at the exit  
250 from mitosis. In the first case, the basic information required for such quick re-establishment is  
251 already present in the sequences of isochores (CTCF may also play an important role in the  
252 process). In the second case, the formation of thousands of loops involves the attachment of loop  
253 extruding factors and an extrusion process, which requires a source of energy. It is obvious that  
254 the first model relying on well known intrinsic physical properties of DNA is to be preferred to  
255 the second one, which involves the interaction of thousands of conjectural loop extruders and an  
256 unknown source of energy.

257 A final point should be made to stress that the models under discussion here concern the  
258 basic evolutionarily stable chromatin domains, since, as it is well known, epigenetic  
259 modifications and environmental factors may cause changes in chromatin architecture; indeed,  
260 while self-associating domains are stable in mammals, chromatin interactions within and between

261 domains may change during differentiation (49) and evolution (the latter subject will be  
262 discussed elsewhere).

263

264 *Isochores as functional genome units*

265 The present results lead to a new vision of isochores since they not only correspond to a  
266 fundamental level of genome structure and organization (50), but also to a set of functional  
267 genome units that encode and mold LADs and TADs. Several observations support the above  
268 conclusion, three of which are the following: 1) the evolutionary conservation of the isochore  
269 patterns in mammals (32); 2) TADs from cells of adult organisms are basic units of replication  
270 timing (51) and GC-rich and GC-poor isochores are replication units characterized by all early or  
271 all late replicons (52); 3) alterations of the architecture of chromatin domains (both LADs and  
272 TADs), known to lead to senescence and diseases (see the review papers cited in the  
273 Introduction), are due to changes in their isochore framework. This was predicted by previous  
274 investigations on “genomic diseases” (53,54), defined as diseases due to sequence alterations that  
275 do not affect genes or classical regulatory sequences, but other sequences that “cause regional  
276 changes in chromatin structure”.

277 The fact that alterations in the chromatin architecture, not affecting genes or classical  
278 regulatory sequences, lead to problems in transcription 1) represents the strongest and final  
279 objection to the idea of “junk DNA” (see ref. 55, for a review); and 2) has practical implications:  
280 indeed, screening even a small human population in terms of chromatin structure in view of  
281 detecting “genomic diseases” is simply not feasible at least at the present time. The availability of  
282 LADs and TADs maps along sequenced human chromosomes may allow, however, to link  
283 alterations at the DNA sequence level with chromatin structure alterations. For instance, the maps

284 of insertions, deletions and SNPs of Venter's chromosomes (56) in combination with reference  
285 chromatin structure maps, might lead to detect problems in Venter's chromatin domains.

286

287 *The large-scale organization of the human genome*

288 We can now consider a higher level of isochore and chromatin organization. At the DNA  
289 level, two "genome spaces" were defined on the basis of gene density (57,58): the gene-poor  
290 "genome desert" (L1+L2 isochores) and the gene-rich "genome core" (H1+H2+H3 isochores). In  
291 the interphase nucleus, the chromatin corresponding to the genome core showed an internal  
292 location and an open structure, whereas the chromatin corresponding to the genome desert  
293 showed a peripheral location and a closed structure (see Table 1); moreover, the former showed a  
294 preference for (generally GC rich) telomeric regions, the latter for centromeric regions, this  
295 preference explaining the polarity of chromosomes in the nucleus (59,60).

296 The recently proposed chromosome compartments, A and B, characterized by open and  
297 closed chromatin, respectively (15), show properties very similar to those just described. In  
298 conclusion, the two compartments, A and B (see the compartment profile of chromosome 21 in  
299 Fig. 4D) appear to correspond to the two genome spaces, the "genome core" and the "genome  
300 desert" (see Table 1). This conclusion is supported by the comparison of sub-compartments with  
301 isochore profiles (26).

302

303 *The genomic code*

304 The encoding of chromatin domains by isochores deserves the name of "genomic code".  
305 This definition was originally coined (61,62; see also ref. 25) for two sets of compositional  
306 correlations 1) those that hold among genome sequences (for instance, between coding and  
307 contiguous non-coding sequences) and among the three codon positions of genes and that reflect

308 isochore properties; and 2) those that link isochores with all the structural/functional properties of  
309 the genome (25,26,31), the latter now including the properties of TADs and LADS. Here it is  
310 proposed that the definition of “genomic code” be applied to the encoding of chromatin domains  
311 by isochores, since this is in fact the basis for the second set of the correlations just mentioned.  
312 Interestingly, the genomic code may be visualized as the fourth, and last, pillar of molecular  
313 biology, the first one being the double helix (1951-1953), the second the regulation of gene  
314 expression in *E. coli* (1957-1961), and the third the genetic code (1961-1966). In contrast with  
315 the other pillars, the genomic code took decades to be established.

316

### 317 **Acknowledgements**

318 The author thanks Paolo Ascenzi for hospitality, Giacomo Bernardi, Oliver Clay, and,  
319 especially, Kamel Jabbari for critical reading, comments and discussions as well as Caterina  
320 Nuvoli for excellent technical help. This research was supported by the Kimura Prize for  
321 Molecular Evolution and Evolutionary Genomics conferred to the author (Tokyo, June 2016).

322

323

324 **References:**

- 325 1. Guelen L, Pagie L, Brasset E, Meuleman W, Faza MB, Talhout W, et al. Domain organization of  
326 human chromosomes revealed by mapping of nuclear lamina interactions. *Nature*. 2008;453:  
327 948–51.
- 328 2. Meuleman W, Peric-Hupkes D, Kind J, Beaudry JB, Pagie L, Kellis M, et al. Constitutive  
329 nuclear lamina-genome interactions are highly conserved and associated with A/T-rich sequence.  
330 *Genome Res*. 2013;23: 270–280.
- 331 3. Kind J, Pagie L, De Vries SS, Nahidiazar L, Dey SS, Bienko M, et al. Genome-wide Maps of  
332 Nuclear Lamina Interactions in Single Human Cells. *Cell*. 2015;163: 134–147.
- 333 4. Dixon JR, Selvaraj S, Yue F, Kim A, Li Y, Shen Y, et al. Topological domains in mammalian  
334 genomes identified by analysis of chromatin interactions. *Nature*. 2012;485: 376–380.
- 335 5. Nora EP, Lajoie BR, Schulz EG, Giorgetti L, Okamoto I, Servant N, et al. Spatial partitioning  
336 of the regulatory landscape of the X-inactivation centre. *Nature*. 2012;485: 381–385.
- 337 6. Rao SSP, Huntley MH, Durand NC, Stamenova EK, Bochkov ID, Robinson JT, et al. A 3D map  
338 of the human genome at kilobase resolution reveals principles of chromatin looping. *Cell*.  
339 2014;159: 1665–1680.
- 340 7. Vietri Rudan M, Barrington C, Henderson S, Ernst C, Odom DT, Tanay A, et al. Comparative  
341 Hi-C Reveals that CTCF Underlies Evolution of Chromosomal Domain Architecture. *Cell Rep*.  
342 2015;10: 1297–1309.
- 343 8. Bonev B, Cavalli G. Organization and function of the 3D genome. *Nat Rev Genet*. *Nature*  
344 *Research*; 2016;17: 661–678.
- 345 9. Dixon JR, Gorkin DU, Ren B. Chromatin Domains: The Unit of Chromosome Organization. *Mol*  
346 *Cell*. 2016;62: 668–680.
- 347 10. Ghirlando R, Felsenfeld G. CTCF: Making the right connections. *Genes and Development*. 2016.  
348 pp. 881–891.
- 349 11. Gonzalez-Sandoval A, Gasser SM. On TADs and LADs: Spatial Control Over Gene Expression.  
350 *Trends Genet*. 2016;
- 351 12. Merckenschlager M, Nora EP. CTCF and Cohesin in Genome Folding and Transcriptional Gene  
352 Regulation. *Annu Rev Genomics Hum Genet*. 2016;17: annurev-genom-083115-022339.

- 353 13. Poeschel R, Coraggio F, Meister P, Ahmed K, Dehghani H, Rugg-Gunn P, et al. From single  
354 genes to entire genomes: the search for a function of nuclear organization. *Development*. Oxford  
355 University Press for The Company of Biologists Limited; 2016;143: 910–23.
- 356 14. Solovei I, Thanisch K, Feodorova Y. How to rule the nucleus: divide et impera. *Curr Opin Cell*  
357 *Biol*. 2016;40: 47–59.
- 358 15. Lieberman-Aiden E, van Berkum NL, Williams L, Imakaev M, Ragooczy T, Telling A, et al.  
359 Comprehensive mapping of long-range interactions reveals folding principles of the human  
360 genome. *Science*. 2009;326: 289–93.
- 361 16. Alipour E, Marko JF. Self-organization of domain structures by DNA-loop-extruding enzymes.  
362 *Nucleic Acids Res*. Oxford University Press; 2012;40: 11202–12.
- 363 17. Barbieri M, Chotalia M, Fraser J, Lavitas LM, Dostie J, Pombo A, et al. Complexity of chromatin  
364 folding is captured by the strings and binders switch model. *Proc Natl Acad Sci U S A*. 2012;109:  
365 16173–16178.
- 366 18. Fudenberg G, Imakaev M, Lu C, Goloborodko A, Abdennur N, Mirny LA. Formation of  
367 Chromosomal Domains by Loop Extrusion. *Cell Rep*. 2016;15: 2038–2049.
- 368 19. Sanborn AL, Rao SSP, Huang S-C, Durand NC, Huntley MH, Jewett AI, et al. Chromatin  
369 extrusion explains key features of loop and domain formation in wild-type and engineered  
370 genomes. *Proc Natl Acad Sci USA*. National Acad Sciences; 2015;112: E6456–E6465.
- 371 20. Dekker J, Mirny L. The 3D Genome as Moderator of Chromosomal Communication. *Cell*.  
372 2016;164: 1110–1121.
- 373 21. Di Pierro M, Zhang B, Aiden EL, Wolynes PG, Onuchic JN. Transferable model for  
374 chromosome architecture. *Proc Natl Acad Sci*. 2016; 201613607.
- 375 22. Rowley MJ, Corces VG. The three-dimensional genome: Principles and roles of long-distance  
376 interactions. *Current Opinion in Cell Biology*. 2016. pp. 8–14.
- 377 23. Ulianov S V, Khrameeva EE, Gavrilov AA, Flyamer IM, Kos P, Mikhaleva EA, et al. Active  
378 chromatin and transcription play a key role in chromosome partitioning into topologically  
379 associating domains. *Genome Res*. Cold Spring Harbor Laboratory Press; 2016;26: 70–84.
- 380 24. Vietri Rudan M, Hadjur S. Genetic Tailors: CTCF and Cohesin Shape the Genome During  
381 Evolution. *Trends Genet*. 2015;31: 651–660.



- 382 25. Bernardi G (2004, reprinted in 2005) *Structural and evolutionary genomics: natural selection in*  
383 *genome evolution*. (Elsevier, Amsterdam). This book is freely available at  
384 [www.giorgiobernardi.eu](http://www.giorgiobernardi.eu)
- 385 26. Jabbari K, Bernardi G. An isochore framework underlies chromatin architecture. Plos One  
386 <http://dx.doi.org/10.1371/journal.pone.0168023>
- 387 27. Costantini M, Clay O, Auletta F, Bernardi G. An isochore map of human chromosomes. Genome  
388 Res. 2006;16: 536–541.
- 389 28. Pavlíček A, Paces J, Clay O, Bernardi G. A compact view of isochores in the draft human  
390 genome sequence. FEBS Lett. 2002;511: 165–9.
- 391 29. Pačes J, Zíka R, Pačes V, Pavlíček A, Clay O, Bernardi G. Representing GC variation along  
392 eukaryotic chromosomes. Gene. 2004;333: 135–141.
- 393 30. Cozzi P, Milanesi L, Bernardi G. Segmenting the human genome into isochores. Evol  
394 Bioinforma. 2015;11: 253–261.
- 395 31. Bernardi G. Chromosome architecture and genome organization. PLoS One. 2015;10.  
396 doi:10.1371/journal.pone.0143739
- 397 32. Costantini M, Cammarano R, Bernardi G. The evolution of isochore patterns in vertebrate  
398 genomes. BMC Genomics. 2009;10: 146. doi:10.1186/1471-2164-10-146
- 399 33. Costantini M, Bernardi G. The short-sequence designs of isochores from the human genome.  
400 Proc Natl Acad Sci U S A. 2008;105: 13971–6.
- 401 34. Meunier-Rotival M, Soriano P, Cuny G, Strauss F, Bernardi G. Sequence organization and  
402 genomic distribution of the major family of interspersed repeats of mouse DNA. Proc Natl Acad  
403 Sci U S A. 1982;79: 355–9.
- 404 35. Soriano P, Meunier-Rotival M, Bernardi G. The distribution of interspersed repeats is  
405 nonuniform and conserved in the mouse and human genomes. Proc Natl Acad Sci U S A.  
406 1983;80: 1816–20.
- 407 36. Varriale A, Bernardi G. Distribution of DNA methylation, CpGs, and CpG islands in human  
408 isochores. Genomics. 2010;95: 25–28.
- 409 37. Arhondakis S, Auletta F, Bernardi G. Isochores and the regulation of gene expression in the  
410 human genome. Genome Biol Evol. 2011;3: 1080–9.

- 411 38. Vinogradov AE. DNA helix: The importance of being GC-rich. *Nucleic Acids Research*. 2003.  
412 pp. 1838–1844.
- 413 39. Di Filippo M, Bernardi G. Mapping DNase-I hypersensitive sites on human isochores. *Gene*.  
414 2008;419:62-65.
- 415 40. Thurman RE, Rynes E, Humbert R, Vierstra J, Maurano MT, Haugen E, et al. The accessible  
416 chromatin landscape of the human genome. *Nature*. 2012;489: 75–82.
- 417 41. Fenouil R, Cauchy P, Koch F, Descostes N, Cabeza JZ, Innocenti C, et al. CpG islands and GC  
418 content dictate nucleosome depletion in a transcription-independent manner at mammalian  
419 promoters. *Genome Res*. 2012;22: 2399–2408.
- 420 42. Naughton C, Avlonitis N, Corless S, Prendergast JG, Mati IK, Eijk PP, et al. Transcription forms  
421 and remodels supercoiling domains unfolding large-scale chromatin structures. *Nat Struct Mol*  
422 *Biol*. 2013;20: 387–95.
- 423 43. Benedetti F, Dorier J, Burnier Y, Stasiak A. Models that include supercoiling of topological  
424 domains reproduce several known features of interphase chromosomes. *Nucleic Acids Res*.  
425 2014;42: 2848–55.
- 426 44. Kaplan N, Moore IK, Fondufe-Mittendorf Y, Gossett AJ, Tillo D, Field Y, et al. The DNA-  
427 encoded nucleosome organization of a eukaryotic genome. *Nature*. 2009;458: 362–366.
- 428 45. Frenkel ZM, Bettecken T, Trifonov EN. Nucleosome DNA sequence structure of isochores.  
429 *BMC Genomics*. 2011;12: 203.
- 430 46. Nora EP, Lajoie BR, Schulz EG, Giorgetti L, Okamoto I, Servant N, et al. Target degradation of  
431 CTCF decouples local insulation of chromosome domains from higher-order genome  
432 compartmentalization. doi: <https://doi.org/10.1101/095802>
- 433 47. Kubo N, Ishii H, Gorkin D, Meitinger F, Xiong X, Fang R, et al. Preservation of Chromatin  
434 Organization after Acute Loss of CTCF in Mouse Embryonic Stem Cells. *bioRxiv*. Cold Spring  
435 Harbor Labs Journals; 2017; 118737.
- 436 48. Uusküla-Reimand L, Hou H, Samavarchi-Tehrani P, Rudan MV, Liang M, et al. Topoisomerase  
437 II beta interacts with cohesin and CTCF at topological domain borders. *Genome Biol*. 2016; 17:  
438 1–22.
- 439 49. Dixon JR, Jung I, Selvaraj S, Shen Y, Antosiewicz-Bourget JE, Lee AY, et al. Chromatin  
440 architecture reorganization during stem cell differentiation. *Nature*. 2015;518: 331–336.

- 441 50. Bernardi G, Olofsson B, Filipski J, Zerial M, Salinas J, Cuny G, et al. The mosaic genome of  
442 warm-blooded vertebrates. *Science*. American Association for the Advancement of Science;  
443 1985;228: 953–8.
- 444 51. Rivera-Mulia JC, Gilbert DM. Replicating Large Genomes: Divide and Conquer. *Mol Cell*.  
445 2016;62: 756–765.
- 446 52. Costantini M, Bernardi G. Replication timing, chromosomal bands, and isochores. *Proc Natl*  
447 *Acad Sci U S A*. 2008;105: 3433–3437.
- 448 53. Bernardi G. The neoselectionist theory of genome evolution. *Proc Natl Acad Sci U S A*.  
449 2007;104: 8385–90.
- 450 54. Al Mahmud A, Amore G, Bernardi G. Compositional genome contexts affect gene expression  
451 control in sea urchin embryo. *PLoS One*. 2008;3. doi:10.1371/journal.pone.0004025
- 452 55. Palazzo AF, Gregory TR. The Case for Junk DNA. *PLoS Genet*. 2014;10.  
453 doi:10.1371/journal.pgen.1004351
- 454 56. Costantini M, Bernardi G. Mapping insertions, deletions and SNPs on Venter’s chromosomes.  
455 *PLoS One*. 2009;4. doi:10.1371/journal.pone.0005972
- 456 57. Bernardi G. The Vertebrate Genome : Isochores and Evolution. *Mol Biol Evol*. 1993;10: 186–  
457 204.
- 458 58. Bernardi G. Isochores and the evolutionary genomics of vertebrates. *Gene*. 2000. 3–17.
- 459 59. Sadoni N, Langer S, Fauth C, Bernardi G, Cremer T, Turner BM, et al. Nuclear organization of  
460 mammalian genomes: Polar chromosome territories build up functionally distinct higher order  
461 compartments. *J Cell Biol*. 1999;146: 1211–1226.
- 462 60. Saccone S, Federico C, Bernardi G. Localization of the gene-richest and the gene-poorest  
463 isochores in the interphase nuclei of mammals and birds. *Gene*. 2002;300: 169–78.
- 464 61. Bernardi G. Le génome des vertébrés : organisation, fonction et évolution. *Biofutur*. 1990. 94 :  
465 43-46.
- 466 62. Bernardi G, Bernardi G. Compositional properties of nuclear genes from cold-blooded  
467 vertebrates. *J. Mol. Evol*. 1986. 33:57-67.
- 468 63. Naumova N, Imakaev M, Fudenberg G, Zhan Y, Lajoie BR, Mirny LA, et al. Organization of the  
469 mitotic chromosome. *Science*. 2013;342: 948–53.

- 470 64. Consortium IHGS. Initial sequencing and analysis of the human genome. *Nature*. 2001;409: 860–  
471 921.
- 472 65. Bernardi G. Misunderstandings about isochores. Part 1. *Gene*. 2001. pp. 3–13.
- 473 66. Jabbari K, Nürnberg P. A genomic view on epilepsy and autism candidate genes. *Genomics*.  
474 2015. 108:31-36.
- 475
- 476

477 **Figure Legends**

478 **Figure 1. A:** Compositional profile (from ref. 30) of human chromosome 21 (release hg38) as seen  
479 through non-overlapping 100-Kb windows. DNA stretches from isochore families L1 to H3 are  
480 represented in different colors, deep blue, light blue, yellow, orange, red, respectively. The left-side  
481 ordinate values are the minima GC values between the isochore families listed on the right side  
482 (see Supplementary Table S1); **a-f** correspond to an H1 peak (**a**) and to several L2<sup>+</sup> peaks (**b** to **f**;  
483 the thin yellow bars in peaks **c**, **e** and **f** correspond to single 100Kb blocks that are assigned to the  
484 H1 family if using “fixed” isochore borders (as shown in the Figure), but to L2 isochores if  
485 “extended” borders (see Supplementary Table 1) are used. Six regions numbered 1 to 6 (top and  
486 bottom of the Figure) of the compositional profile are separated by vertical lines or double lines, X  
487 and Y.

488 **B.** Isochore profile of human chromosome 21 using the matched b37 assembly of ref. 6 and a  
489 sliding window approach (28,29) with “fixed” isochore borders (from ref. 26). The color  
490 convention is as in Fig. 1A. This profile is slightly more extended on the centromeric (left) side  
491 than that of Figs. 1A and 1C.

492 **C.** Isochore profile of human chromosome 21 (release hg38) using a non-overlapping 100Kb  
493 window and the isoPlotter program (from ref. 30).

494 **D.** GC levels of 100Kb windows of human chromosome 21. This figure shows that individual  
495 isochores from the L2<sup>+</sup> to H3 families are in the form of peaks. The GC gradients of the peaks do  
496 not appear in a clear way in the standard presentation of compositional profiles of chromosomes  
497 (Fig. 1A), except for the broad, isolated H1 (**a**) and L2<sup>+</sup> peaks (**b** to **f**). Upon close inspection,  
498 however, the peaks of the H1, H2 and H3 isochores of this Figure show a correspondence with the  
499 small peaks of isochores belonging to H1, H2 and H3 family present in Fig. 1B. Blue and red

500 arrows delimit regions 2 and 6, respectively. Black, blue and red arrows, as well as X,Y double  
501 lines (see Fig. 4 and its legend for additional information) separate regions 3,4 and 5; horizontal  
502 lines correspond to minima GC values between isochore families (see legend of Fig. 1A and  
503 Supplementary Table 1).

504 **E.F.** The compositional map of a 2.1Mb region of human chromosome 20, using a sliding window  
505 approach (from ref. 28) and the “extended” family borders of Supplementary Table 1 (Fig. 1E), is  
506 aligned with the corresponding “point-by-point map” (Fig. 1F, in the Fig. 1D style). The  
507 correspondence of five peaks and valleys from the latter (red lines) precisely correspond to the  
508 peaks and valleys of the compositional profile; several additional peaks and valleys show a less  
509 precise, yet unequivocal correspondence (blue lines). The GC range of the peaks from the bottom  
510 profile, 1F, is much larger (about double) than the corresponding one of the top profile, 1E. The  
511 whole region may be visualized as a multipeak H2 isochore on the basis of the bottom profile (see  
512 also Supplementary Fig. S3).

513

514 **Figure 2A.** GC levels of 100Kb windows from L1 and H3 regions of human chromosome 21  
515 comprised between the blue and red arrows (regions 2 and 6) of Fig. 1D, respectively, are  
516 displayed at a higher magnification. Horizontal lines correspond to “fixed” minima GC values  
517 between isochore families (see Supplementary Table 1). The abscissa scale is in 100Kb units.

518 **B.C.** GC levels of 100Kb windows from the regions 1,3,4 and 5 of human chromosome 21. See the  
519 legend of Fig. 2A for other indications. **C.** Region 4 is delimited by two GC-poor sequences, X and  
520 Y, that correspond to LADs (see Fig. 4 and its legend for additional information).

521

522 **Figure 3. A.** The isochore profile of human chromosome 21 is compared with the (inverted) LAD  
523 profile (from ref. 3) to show the correspondence of LADs 1) with L1 isochores (blue lines; two  
524 broken blue lines bracket the largest L1 isochore, in which case the LAD is (exceptionally)  
525 interrupted by an interLAD); 2) with one L2 “valley” isochore (blue line, last on the right side);  
526 and 3) with two LADs flanking the centromere. Four “high heterogeneity” L2<sup>+</sup> “peak” isochores  
527 (red lines) correspond to interLADs, or TADs; the H1 peak right of the centromere corresponds to  
528 the same interLAD as the first L2<sup>+</sup> peak. Two LADs flank the centromere. The multicolored bar on  
529 the right is the color code for isochore families.

530 **B.** The isochore profile of human chromosome 20 (see also legend of Fig. 3A) is compared with  
531 the (inverted) LAD profile (from ref. 3) to show the correspondence of LADs with a large low-  
532 heterogeneity L2 (L2<sup>-</sup>) isochore (bracketed by broken blue lines; on the left of the panel) which  
533 includes an interLAD (red line) and with several L2 “valley” isochores (blue lines), as well as the  
534 correspondence of interLADs with GC-rich isochores (red lines); two faint LADs flank the  
535 centromere.

536 **C.** The isochore profile of human chromosome 19 (see also legend of Fig. 3A) is compared with  
537 the (inverted) LAD profile (from ref. 3) to show that two LADs correspond to H1 isochores (blue  
538 lines) flanking a H2 isochore, an interLAD (red line); two other LADs (on the left) correspond to  
539 L2 “valley” isochores (blue lines); two faint LADs flank the centromere.

540 **Figure 4.** The compositional profile of human chromosome 21 (**B**, from Fig. 1D), is compared 1)  
541 with the corresponding LAD profile (**A**; an inverted scale is shown on the top right of the figure);  
542 2) with the heat map of chromatin interactions (**C**; from ref. 26) and with Fig. 1A on the right side;  
543 3) with the A/B compartment profile (**D**; data for mid G1 from ref. 63). Regions 1 and 3  
544 correspond to multiple interactions and to open chromatin; region 2 to multiple interactions and

545 closed chromatin, as well as to an interLAD. Two double vertical black lines, X and Y,  
546 corresponding to LADs (characterized by both self- and intra-chromosomal interactions) and to  
547 closed chromatin separate region 4 a multi-peak H1 isochore block corresponding to multiple  
548 interactions and open chromatin, from regions 3 and 5. The small multi-peak H2 isochores (region  
549 5) corresponds to a single self-interaction (see text) and to open chromatin (see Text). A telomeric  
550 block of H3 isochores (region 6) defined by red points, arrows and lines corresponds to several (at  
551 least three) self-interactions on the heat map and to open chromatin.

552

553 **Figure 5.** Models for the formation of LADs and TADs. Three chromatin fibers are taken into  
554 consideration: **A.** a GC-poor chromatin fiber corresponding to an L1 isochore; blue bar) bounded  
555 by CTCF binding sites (green) attaches to the lamina, forming a LAD; the wavy profile indicates  
556 the physical adaptation by bending and twisting to (and embedding in) the lamina due to  
557 nucleosome depletion associated with oligo-A sequences (yellow stripes), as well as the self-  
558 interactions. **B.** a GC-rich chromatin fiber corresponding to an H3 isochore folds upon itself  
559 forming a single-loop TAD bounded by CTCF-binding sites (green); yellow to red color indicate  
560 an increasing GC level which is responsible for the folding due to nucleosome depletion associated  
561 with increasing GC, CpG islands and Alu sequences. **C.** A GC-rich chromatin fiber corresponding  
562 to an H1 (or H2) isochore characterized by two GC peaks folds to form a TAD which comprises  
563 two loops and two contact domains.

564



565

<b>TABLE 1. GENOME ORGANIZATION: DNA AND CHROMATIN (a)</b>		
<b>2 Genome spaces (57,58)</b>	<b>Genome core GC-rich, gene-rich</b>	<b>Genome desert GC-poor, gene-poor</b>
<b>2 Nuclear locations (59,60)</b>	<b>Internal</b>	<b>Peripheral</b>
<b>2 Chromatin structure (60)</b>	<b>Open</b>	<b>Closed</b>
<b>2 Replication timings (51,52)</b>	<b>Early</b>	<b>Late</b>
<b>2 Genome compartments (15)</b>	<b>A, open chromatin</b>	<b>B, closed chromatin</b>
<b>5 Isochore families (25)</b>	<b>L2<sup>+</sup>, H1, H2, H3</b>	<b>L1, L2<sup>-</sup></b>
<b>2 Chromatin domains (3-7)</b>	<b>TADs</b>	<b>LADs</b>

566

567

568

(a) see heading “The large-scale organization of the Human genome” in the Discussion section of the manuscript for a description of this Table.

569

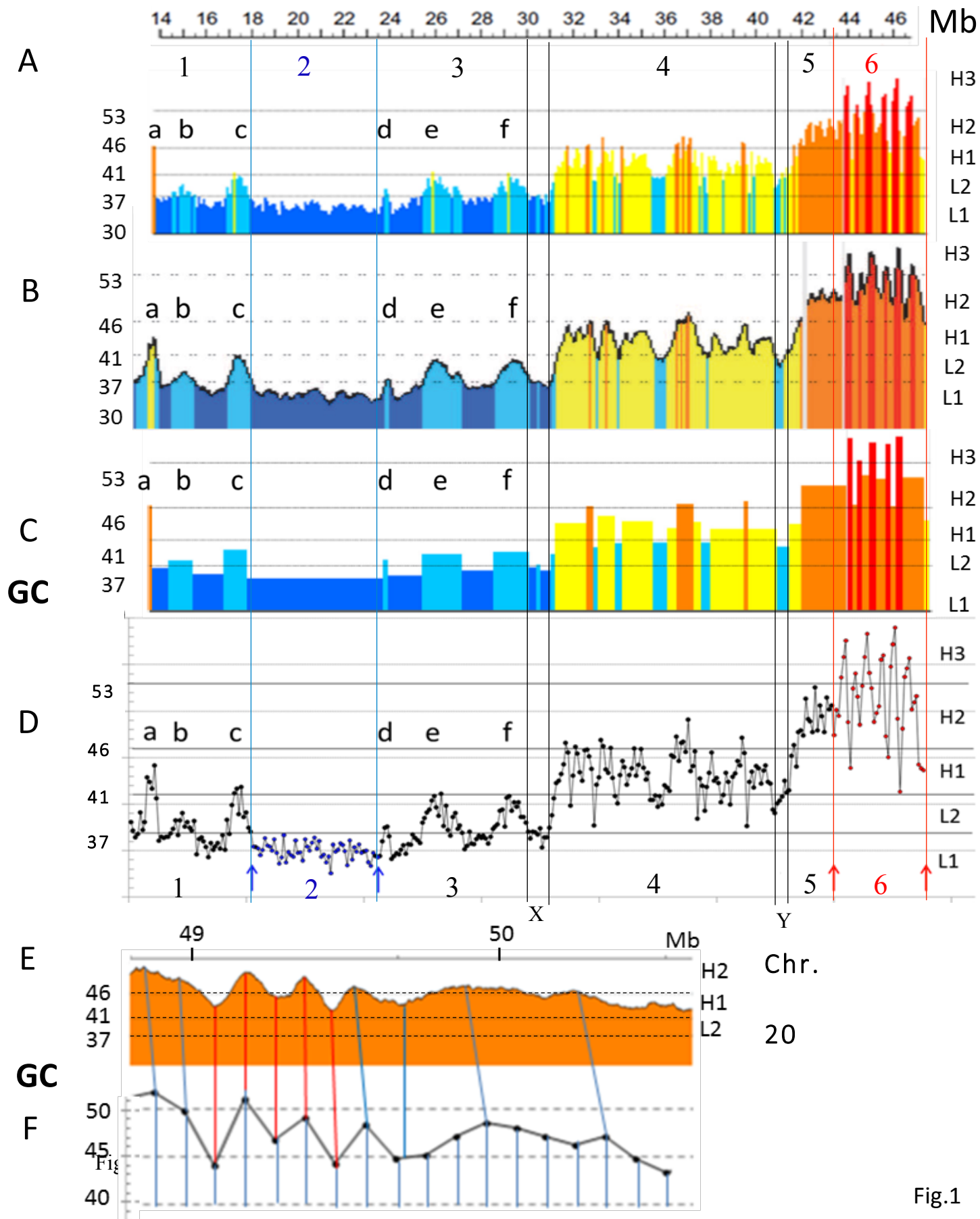


Fig.1

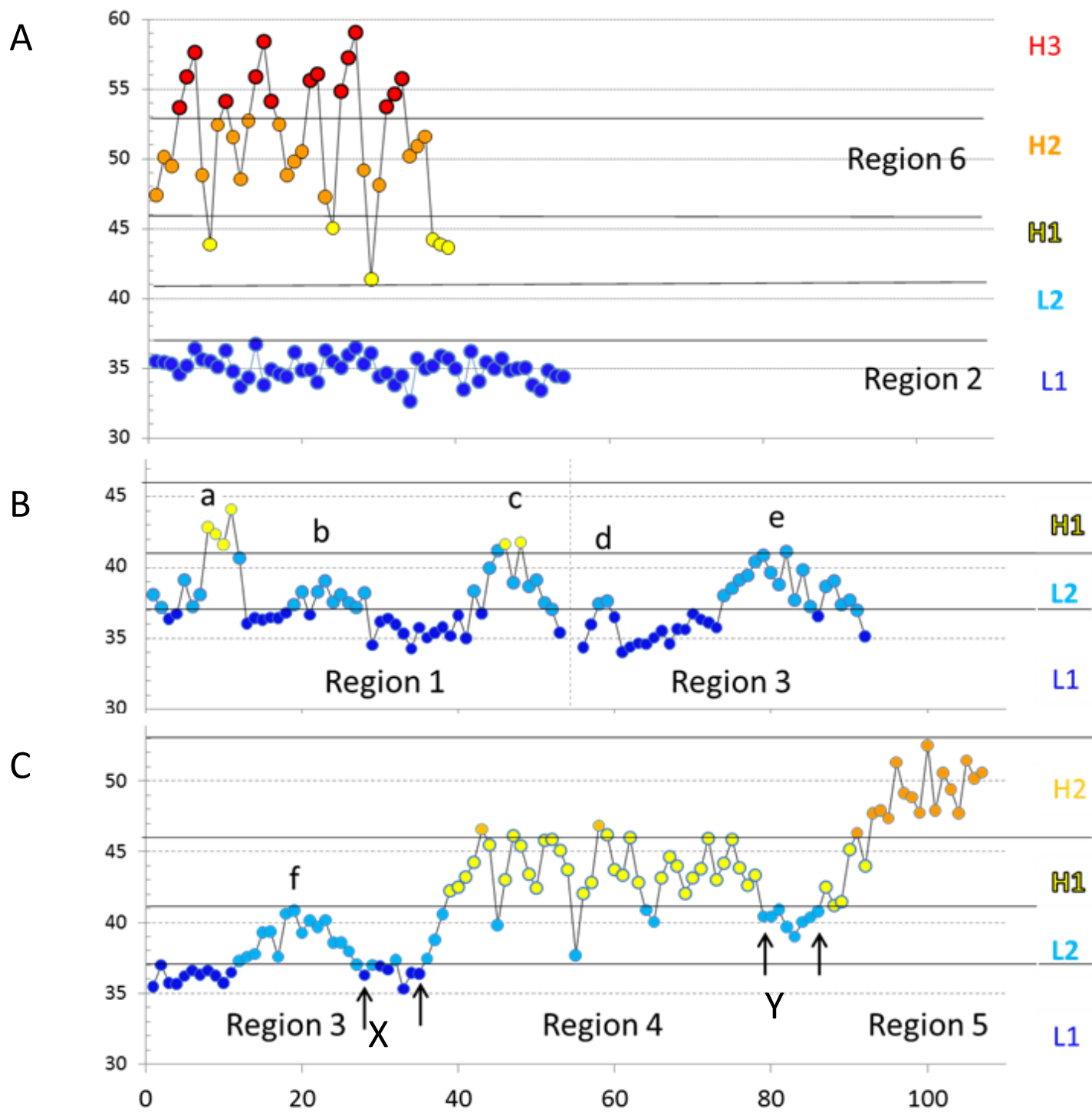


Fig. 2

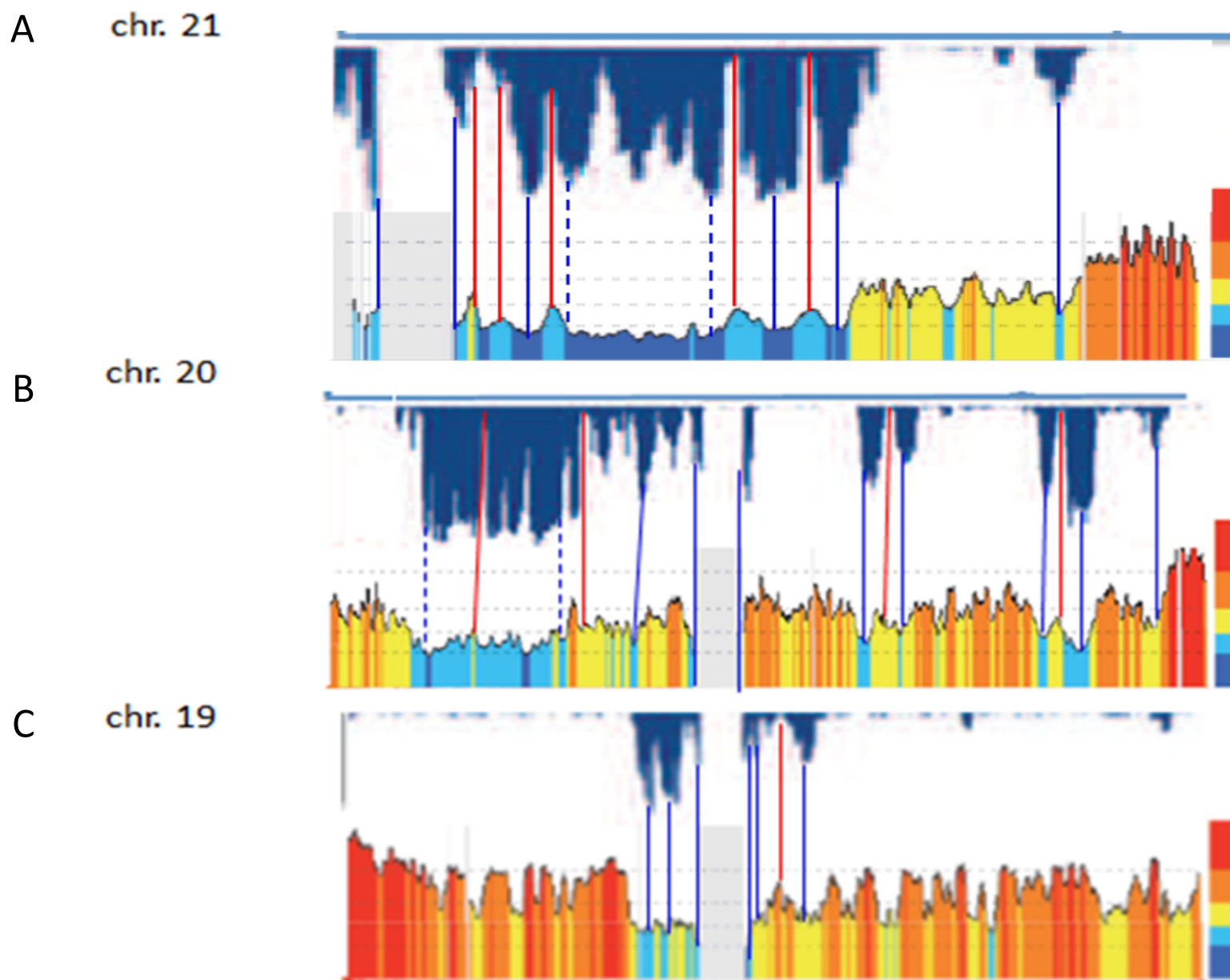


Fig. 3

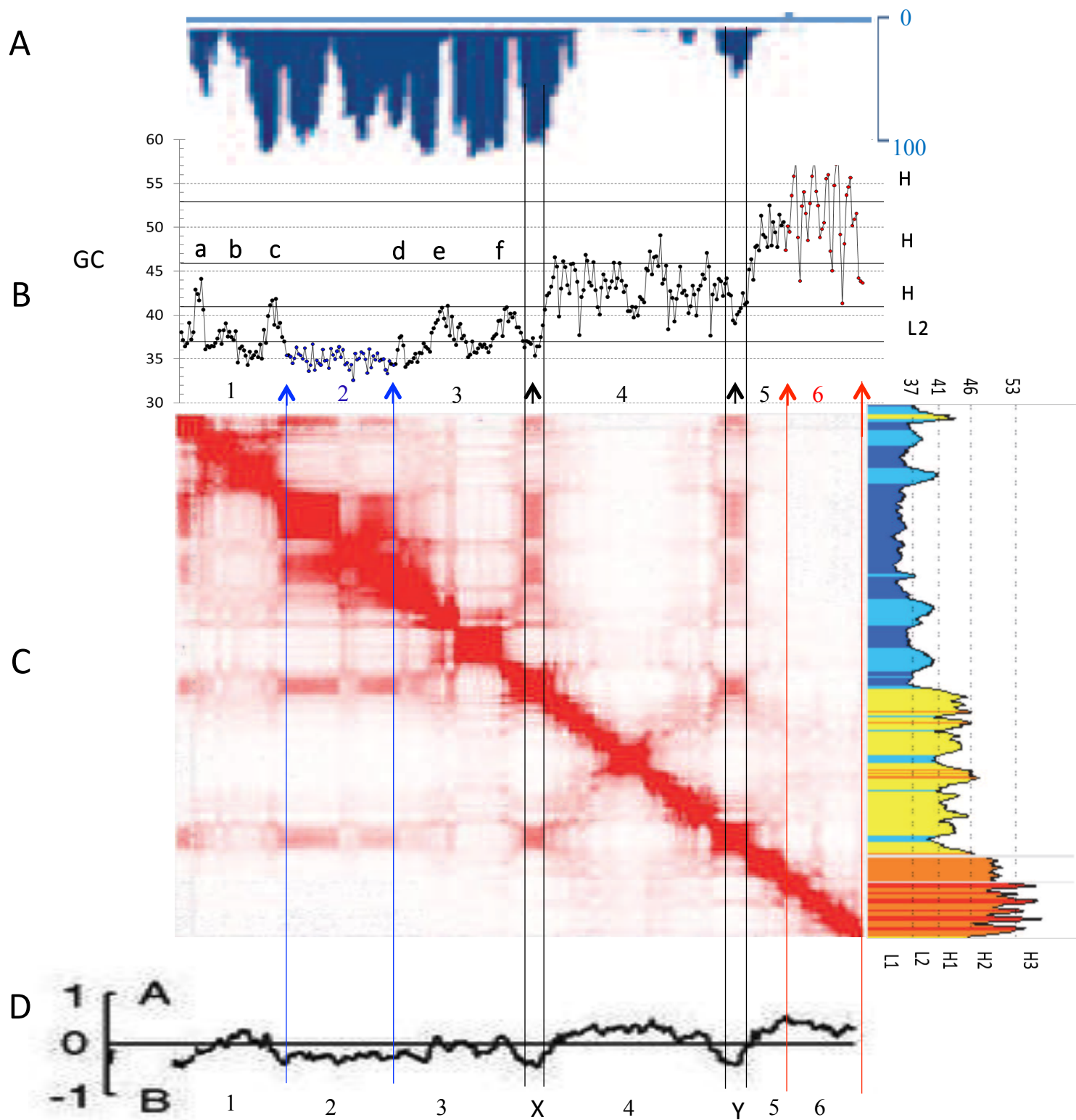


Fig. 4

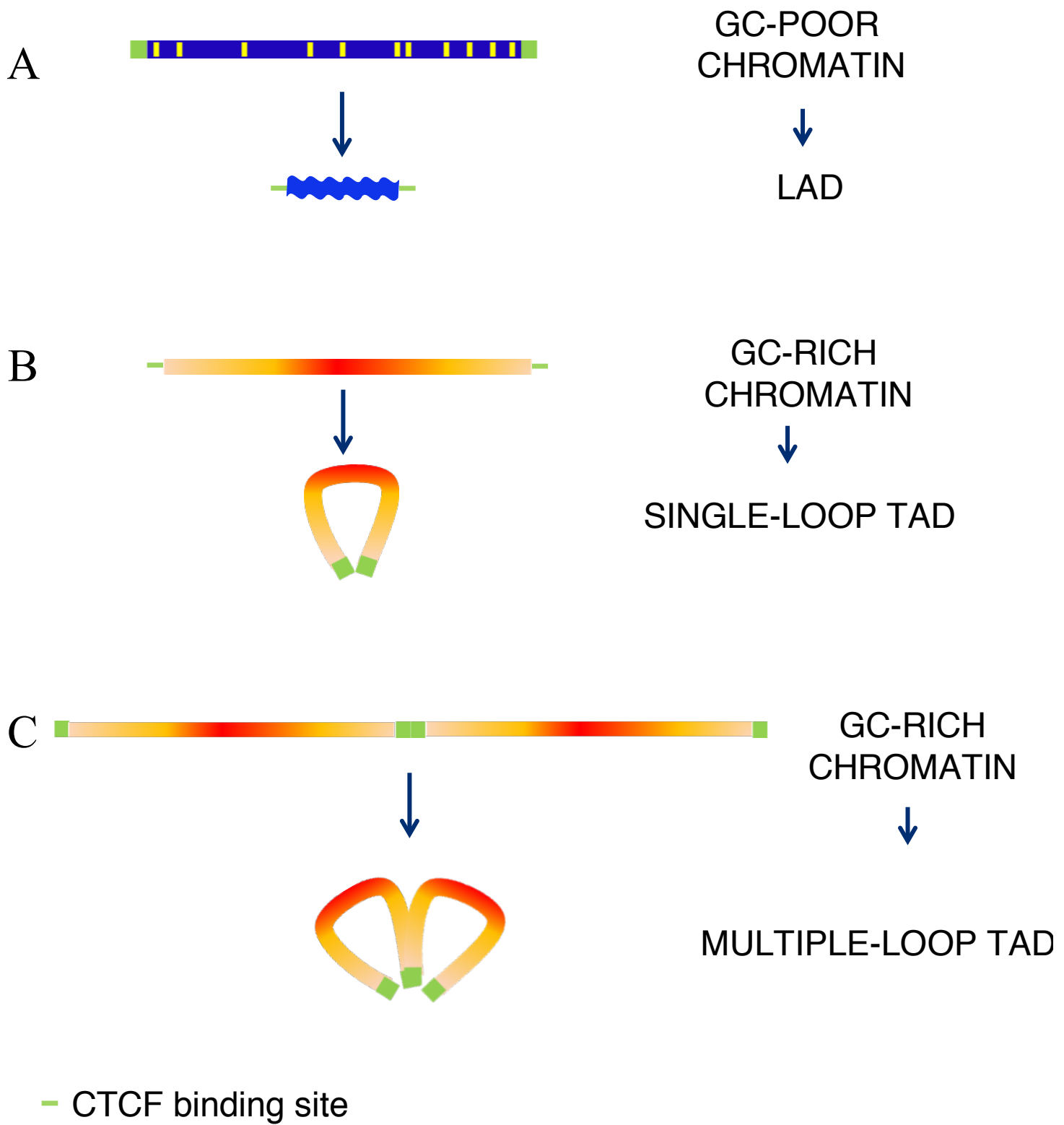


Fig. 5